We are IntechOpen,
the world's leading publisher of
Open Access books
Built by scientists, for scientists

6,900
Open access books available

186,000
International authors and editors

200M
Downloads

Our authors are among the

154
Countries delivered to

TOP 1%
most cited scientists

12.2%
Contributors from top 500 universities

CLARIVATE ANALYTICS

BOOK
CITATION
INDEX

INDEXED

WEB OF SCIENCE™

Selection of our books indexed in the Book Citation Index
in Web of Science™ Core Collection (BKCI)

Interested in publishing with us?
Contact book.department@intechopen.com

Numbers displayed above are based on latest data collected.
For more information visit www.intechopen.com

Characterizing Molecular Rotations using Monte Carlo Simulations

Bart Verberck
University of Antwerp
Belgium

1. Introduction

The Monte Carlo (MC) simulation technique is a powerful method for calculating thermodynamic averages of physical quantities of many-body systems. The physical property we focus on in this Chapter is molecular rotational motion. The rotational degrees of freedom in molecular crystals give rise to temperature- and/or pressure-driven transitions between phases with freely rotating, quasi-freely rotating, or orientationally ordered molecules. Orientationally disordered crystals represent a state of matter between the liquid and the purely crystalline state, and can be compared to liquid crystals. In liquid crystals, however, translational order is destroyed and orientational order is preserved, while in molecular crystals translational order persists while molecules are (partially) orientationally disordered. For a review on molecular crystals we refer to Lynden-Bell & Michel (1994). The molecular crystals we envisage can be as simple as solid hydrogen, but as complex as protein crystals. Also, we do not restrict ourselves to crystals containing only one type of molecule, or to three-dimensional (3D) molecular arrangements. An example of a heterogeneous molecular crystal is fullerene-cubane, $C_{60}.C_8H_8$, while fullerene molecules like C_{60} or C_{70} packed inside a carbon nanotube (CNT) provide an instance of a one-dimensional (1D) molecular chain.

MC simulations provide an excellent tool for the computational study of the different phases, and the transitions between them, of molecular crystals. First, molecular crystals typically consist of molecules interacting via van der Waals interactions, which can be relatively easy modeled using phenomenological potential models. Secondly, the main advantage of MC simulations is the possibility to directly change pressure and temperature, and to examine how the crystal's structure (from the point of view of molecular order/disorder) changes accordingly.

While the actual implementation of molecular rotations in (MC) simulations is typically covered in textbooks, e.g. Allen & Tildesley (1987) and Frenkel & Smit (2002), the actual characterization of molecular rotations and orientations has received much less attention. In this Chapter, we present a method to assess molecular rotational motion within molecular crystals based on the concept of orientational mean-squared displacements (OMSDs). The technique provides an efficient way for describing different rotational regimes of individual molecules and of the molecular crystal as a whole. From a computational point of view, the method has the advantage that only a limited number of parameters has to be sampled and stored to obtain the necessary information on molecular motion and ordering.

We consider rigid molecules, so that each molecule has three translational and three rotational degrees of freedom. The context of the present Chapter assumes a fully set-up MC simulation of a system of molecules, in any ensemble, with all the usual ingredients like interaction

potentials, periodic boundary conditions, minimum-image convention, trial moves, etc. included. In the next section, we formally define OMSDs and demonstrate how they can be used to quantify molecular motion. In Sect. 3, we turn to the practical implementation of the OMSD method. We also recall how to perform rotational MC trial moves and provide a memory-efficient way of doing simulation runs. Next (Sect. 4), we present two examples where OMSDs have been used to extract information on molecular orientations. In Sect. 5 we provide a Chapter summary.

2. OMSDs: general formulation

2.1 Definition

During a MC simulation, a sequence of orientations is generated for every molecule. To fix ideas, let us focus on one type of molecule. The concepts introduced here are easily generalizable to multi-component molecular crystals. As a molecule adopts various orientations, for any point $\vec{r}_i$ fixed with respect to the molecule, e.g. an atom or a bond (when speaking of a bond and its coordinates, the center of the bond is understood), a set of locations $\{\vec{r}_i(p), p = 1, \ldots, P\}$ is produced. Here, i labels the considered molecule, p labels subsequent MC steps and P is the total number of MC samples. The coordinates $\vec{r}_i = (x_i, y_i, z_i)$ of this "monitored" point are defined with respect to the local cartesian system of axes (o, x, y, z), where the origin o coincides with the molecule's center of mass, and the axes (x, y, z) are fixed and parallel to the global coordinate system's axes (X, Y, Z).

For a freely rotating molecule, the set $\{\vec{r}_i(p)\}$ eventually (for $P \longrightarrow \infty$) covers a sphere with radius $|\vec{r}_i|$. If we consider the same monitored point for every molecule, $|\vec{r}_i| \equiv r$ is independent of the molecular index i. In fact, it is advisable to use the same monitored point for every molecule, and we will work under this assumption throughout the whole Chapter. If the molecule does not rotate at all, $\vec{r}_i(p) \equiv \vec{r}_i$ is constant. In Fig. 1, the example of a rotating square is shown, with the middle point of one of the edges as the monitored point.
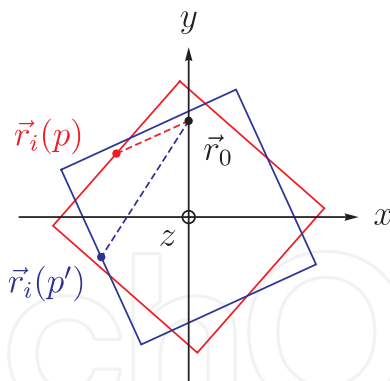

Fig. 1. Two configurations p and p' of a rotating square. The middle point of one of the edges is chosen as the monitored point $\vec{r}_i$, the fixed point $\vec{r}_0$ lies on the y-axis. When the square adopts various orientations, the distance $u_i = |\vec{r}_i - \vec{r}_0|$ between $\vec{r}_i$ and $\vec{r}_0$ (dashed lines) varies accordingly. If the square rotates freely in three dimensions, the monitored point $\vec{r}_i$ describes a sphere with radius $|\vec{r}_i|$.

The idea behind OMSDs is to calculate for every molecule, after each MC step, the square of the distance $u_i(p)$ between the monitored point $\vec{r}_i(p)$ and a fixed point $\vec{r}_0 = (x_0, y_0, z_0)$:

$$u_i(p)^2 = |\vec{r}_i(p) - \vec{r}_0|^2 = \left[x_i(p) - x_0\right]^2 + \left[y_i(p) - y_0\right]^2 + \left[z_i(p) - z_0\right]^2. \tag{1}$$

The fixed point $\vec{r}_0$ has to be defined with respect to the local coordinate system (o, x, y, z) associated with the molecule i under consideration. We take the same fixed point for every molecule. In Fig. 1 the fixed point $\vec{r}_0$ is chosen on the y-axis. The OMSD associated with the chosen fixed point is then obtained by averaging over all MC steps:

$$\langle u_i^2 \rangle = \frac{1}{P} \sum_{p=1}^{P} u_i(p)^2. \tag{2}$$

It is also useful to average over all molecules in the system:

$$\langle\langle u^2 \rangle\rangle = \frac{1}{N} \sum_{i=1}^{N} \langle u_i^2 \rangle, \tag{3}$$

with N the total number of molecules. As we will illustrate in Sect. 4, the overall OMSD $\langle\langle u^2 \rangle\rangle$ [Eq. (3)] is a good measure for oriental motion in the system when all molecules rotate simultaneously in a similar way, while the molecular OMSDs $\langle u_i^2 \rangle$ [Eq. (2)] can be used to characterize orientationally ordered phases.

2.2 Characterization of orientational regimes using OMSDs

By carefully choosing the monitored and fixed points, it is possible to compare the numerically obtained OMSDs $\langle u_i^2 \rangle$ with analytically calculated values. As an example, let us choose the point $(0, 0, z_0)$ as the fixed point, and consider three special cases of molecular motion: (i) free three-dimensional (3D) rotation, (ii) free rotation about the z-axis and (iii) no rotation (i.e. a fixed orientation).

Free 3D rotation. The analytical calculation of $\langle u_i^2 \rangle$ is most easily done by introducing spherical coordinates:

$$x_i = r_i \sin\theta_i \cos\phi_i, \tag{4a}$$
$$y_i = r_i \sin\theta_i \sin\phi_i, \tag{4b}$$
$$z_i = r_i \cos\theta_i. \tag{4c}$$

Here, $\vec{r}_i = (x_i, y_i, z_i)$ stands for the monitored point of molecule i. The squared distance u_i^2 then reads

$$u_i^2 = r_i^2 - 2r_i z_0 \cos\theta_i + z_0^2. \tag{5}$$

To calculate the analytical OMSD, we apply the formula for the 3D orientational average of a quantity $f \equiv f(\theta_i, \phi_i)$,

$$\langle f \rangle_a = \frac{1}{4\pi} \int_0^{2\pi} d\phi_i \int_0^{\pi} \sin\theta_i d\theta_i f(\theta_i, \phi_i), \tag{6}$$

for $f = u_i^2$. The result reads

$$\langle u_i^2 \rangle_a = r_i^2 + z_0^2. \tag{7}$$

Here, we write $\langle u_i^2 \rangle_a$ for the analytical result to distinguish it from the numerical result $\langle u_i^2 \rangle$ [Eq. (2)]. The former follows from an integration, the latter from a summation.

Free rotation about the z-axis. In the case of free rotation about the z-axis, the average reads

$$\langle f \rangle_\mathrm{a} = \frac{1}{2\pi} \int_0^{2\pi} d\phi_i f(\phi_i), \tag{8}$$

which for $f = u_i^2$ results in

$$\langle u_i^2 \rangle_\mathrm{a} = r_i^2 - 2r_i z_0 \cos \theta_i + z_0^2. \tag{9}$$

Fixed orientation. If the molecule does not rotate, one simply has

$$\langle f \rangle_\mathrm{a} = f, \tag{10}$$

so that

$$\langle u_i^2 \rangle_\mathrm{a} = r_i^2 - 2r_i z_0 \cos \theta_i + z_0^2. \tag{11}$$

A characterization of molecular motion can be obtained by comparing the numerical and analytical OMSD values, $\langle u_i^2 \rangle$ and $\langle u_i^2 \rangle_\mathrm{a}$, respectively. However, the resulting values do not uniquely define an orientational regime. In the analytical analysis shown above, one finds the same value for free rotation about the z-axis ('free z-rotation') and for no rotation. The remedy for this is to introduce additional fixed points. Repeating the analytical calculation for fixed points $(x_0, 0, 0)$ and $(0, y_0, 0)$ shows that with more than one fixed point, a distinction between the three regimes considered above is possible. The resulting analytical OMSD values for $\vec{r}_0 = (x_0, 0, 0)$, $(0, y_0, 0)$ and $(0, 0, z_0)$ are summarized in Table 1. Note that the use of only $(x_0, 0, 0)$ and $(0, 0, z_0)$ already allows to distinguish between the three proposed rotational regimes, but that the use of only $(x_0, 0, 0)$ and $(0, y_0, 0)$ does not. This shows that it is important to decide beforehand which fixed points to use. To avoid ambiguous situations, it is best to implement the calculation of OMSDs based on three fixed points of the type $(x_0, 0, 0)$, $(0, y_0, 0)$ and $(0, 0, z_0)$.

$\vec{r}_0$	$\langle u_i^2 \rangle_\mathrm{a}$		
	free 3D rotation	free z-rotation	no rotation
$(x_0, 0, 0)$	$r_i^2 + x_0^2$	$r_i^2 + x_0^2$	$r_i^2 - 2r_i x_0 \sin \theta_i \cos \phi_i + x_0^2$
$(0, y_0, 0)$	$r_i^2 + y_0^2$	$r_i^2 + y_0^2$	$r_i^2 - 2r_i y_0 \sin \theta_i \sin \phi_i + y_0^2$
$(0, 0, z_0)$	$r_i^2 + z_0^2$	$r_i^2 - 2r_i z_0 \cos \theta_i + z_0^2$	$r_i^2 - 2r_i z_0 \cos \theta_i + z_0^2$

Table 1. Analytical OMSD values $\langle u_i^2 \rangle_\mathrm{a}$ for three well-chosen fixed points $\vec{r}_0$. Note that for free rotation about the z-axis, the value of θ_i is indeed fixed and not averaged out. Likewise for θ_i and ϕ_i in the case of no rotation.

3. OMSDs: implementation

3.1 Implementation of random rotations in a MC simulation

Whereas performing translational moves of molecules in a MC simulation is straightforward, implementing 3D orientational motion is less trivial. First, molecular orientational jumps in a MC simulation have to be generated in a random way, and secondly, it has to be possible to attribute a controllable amplitude to a rotation. Therefore, the explicit use of Euler rotations is not recommended. Popular modern approaches are based on quaternions — for more details we refer to Allen & Tildesley (1987), Frenkel & Smit (2002) and Vesely (1982). We suggest the following procedure: (i) first select a random unit vector $\vec{s} \equiv (s_x, s_y, s_z)$ originating from the molecule's center of mass and (ii) then rotate the molecule about $\vec{s}$ over α. The angle α is then

a direct measure for the rotional jumps' amplitude and the interval where its value should be randomly selected from can be adjusted — before definitive data collecting — to yield the desired acceptance rate (typically 50%) for rotational MC trial moves.

The generation of a random unit vector in three dimensions $\vec{s} = (\sin\theta\cos\phi, \sin\theta\sin\phi, \cos\theta)$, in other words randomly choosing a point on a sphere with radius 1, is not achieved by choosing uniformly random values for the polar and azimuthal angles θ and ϕ in the intervals $[0, \pi]$ and $[0, 2\pi[$, respectively [Miles (1965)]. (Note that in two dimensions it does suffice to randomly choose ψ between 0 and 2π for $\vec{s} \equiv (s_x, s_y) = (\cos\psi, \sin\psi)$ to be a random unit vector.) The correct recipe reads

$$s_x = \sqrt{1 - q_1^2}\cos q_2, \tag{12a}$$

$$s_y = \sqrt{1 - q_1^2}\sin q_2, \tag{12b}$$

$$s_z = q1, \tag{12c}$$

$$q_1 = 2r_1 - 1, \tag{12d}$$

$$q_2 = 2\pi r_2, \tag{12e}$$

where r_1 and r_2 are random numbers uniformly distributed in the interval $[0, 1[$. Rotating the point $\vec{r} \equiv (x, y, z)$ of the molecule about $\vec{s}$ over α results in the point

$$\vec{r}' = \vec{r}_\parallel + \vec{r}_\perp \cos\alpha + (r_\perp \times \vec{s})\sin\alpha, \tag{13}$$

where

$$\vec{r}_\parallel = (\vec{s}\cdot\vec{r})\vec{r}, \tag{14a}$$

$$\vec{r}_\perp = \vec{r} - \vec{r}_\parallel. \tag{14b}$$

In the more common form of a matrix multiplication, one has

$$\vec{r}' = R_{\vec{s}}(\alpha)\vec{r} \tag{15}$$

with $R_{\vec{s}}(\alpha)$ given by

$$R_{\vec{s}}(\alpha) = \begin{pmatrix} s_x^2(1 - \cos\alpha) + \cos\alpha & s_xs_y(1 - \cos\alpha) + s_z\sin\alpha & s_zs_x(1 - \cos\alpha) - s_y\sin\alpha \\ s_xs_y(1 - \cos\alpha) - s_z\sin\alpha & s_y^2(1 - \cos\alpha) + \cos\alpha & s_ys_z(1 - \cos\alpha) + s_x\sin\alpha \\ s_zs_x(1 - \cos\alpha) + s_y\sin\alpha & s_ys_z(1 - \cos\alpha) - s_x\sin\alpha & s_z^2(1 - \cos\alpha) + \cos\alpha \end{pmatrix}. \tag{16}$$

3.2 Sampling OMSDs. Resetting the monitored point

The following remarks apply generally to any molecular crystal, possibly with several types of molecules in it, but to fix ideas, we take the example of a system of benzene molecules, C_6H_6. Let us consider one molecule, labeled i, and take one of its six C atoms as the monitored point and label that atom C_1. After starting the MC simulation, it is likely that the point C_1 will drift away from its initial position. At equilibrium, the molecule might rotate three-dimensionally, or rotate about an axis, or adopt a fixed orientation. In any case, it is important to start sampling OMSDs only after equilibrium has set in — which applies in fact for all quantities sampled in a MC simulation — since the path the atom C_1 has been describing before equilibrium is bound to bias the outcome of the value of $\langle u_i^2 \rangle$.

A more subtle issue arises from molecular symmetry and the equivalence of points related by symmetry operations. Continuing with the benzene example, we now consider two molecules

i and j, and monitor their C_1 atoms. Again, after the start of the MC simulation, both atoms are likely to drift away from their initial positions. Note that the initial positions can coincide (in the case of identical molecular orientations at initialisation), but that they do not have to (in the case of random molecular orientations at start-up). If, after equilibrium has set in, the molecules adopt the same fixed orientation, it is probable that atom C_1 of molecule i and atom C_1 of molecule j are differently positioned (Fig. 2). This typically occurs upon cooling: at high temperature the molecules rotate, and at low temperature the system is orientationally ordered. In the latter case, different positions of C_1 for molecules i and j result in different OMSD values for molecules i and j, although their orientations are the same.
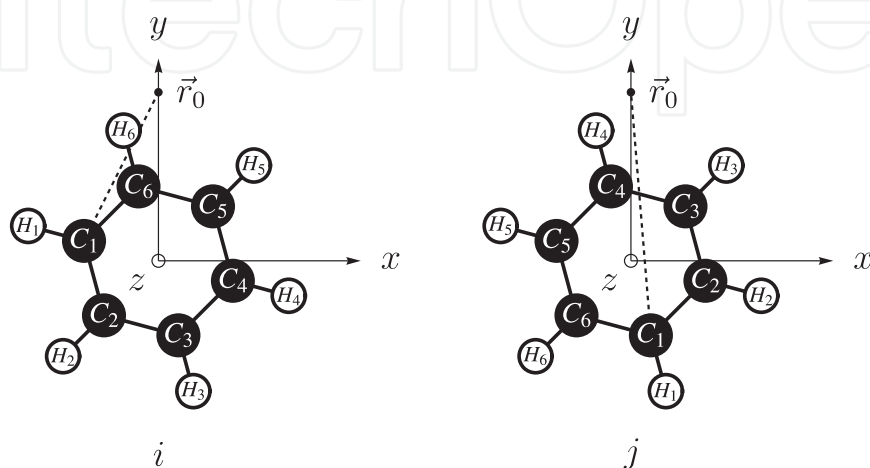

Fig. 2. Benzene molecules i (left) and j (right) in equivalent orientations, but with the atoms C_k and H_k ($k = 1, \ldots, 6$) differently located. With C_1 as the monitored point, the distances u_i and u_j (dashed lines) between the monitored point and the fixed point $\vec{r}_0$ (here chosen on the y-axis) are different.

A remedy for this is to introduce a fixed reference orientation, which we call standard orientation, and to "reset" the monitored point when starting to sample OMSDs. In the present example, we define the standard orientation as the configuration with all atoms in the z-plane, and two C atoms lying on the y-axis (Fig. 3). The C atom with $y > 0$ is labeled C_1 and chosen to be the **reference monitored point**. When equilibrium has set in, the C atom of the molecule — in its present orientation — closest to the C_1 atom of the molecule in the standard orientation is chosen as the **dynamic monitored point** $\vec{r}_i$. In this way, molecular symmetry is accounted for, and different realizations of one molecular configuration result in the same u_i values — and consequently, in the same OMSD values. Note the importance of the choice of a standard orientation, and the dynamic redefinition of the monitored point.

The foregoing is valid for any choice of monitored point — atoms, bonds, or any other locus. Rather than choosing one particular point (e.g. a C atom), a family of equivalent points (e.g. six C atoms) related by symmetry operations (e.g. six-fold rotations about the z-axis) is chosen; the point then actually monitored is the point closest to one of the equivalent points (e.g. C_1) having a precise location for the molecule in the standard orientation. We point out that the reset procedure is required for every molecule in the system.

3.3 Program flow and data management

Having defined OMSDs, discussed how to use them for characterizing rotational regimes, and having made some practical remarks on random rotations and resetting the monitored points, we now turn to a discussion of how to practically include the calculation of OMSDs in
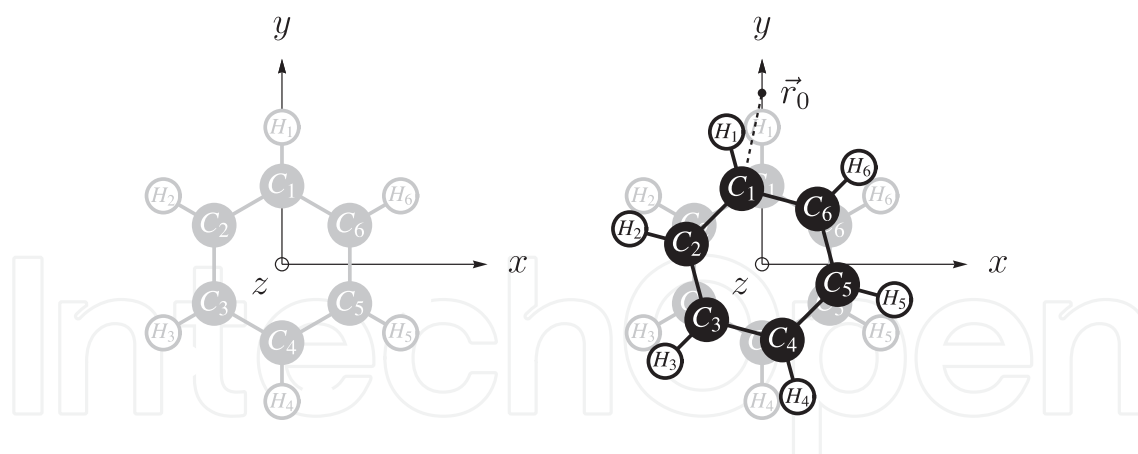
Fig. 3. Benzene molecule in the standard orientation (gray), with the carbon atom labeled C_1 — the reference monitored point — on the y-axis. Resetting the dynamic monitored point is done by identifying the carbon atom closest to the reference monitored point as shown right where the present molecular orientation (black) is superimposed on the standard orientation (gray).

a real MC simulation of a molecular crystal. We also suggest a way to manage the resulting data, with the advantage of limited data storage in combination with unlimited simulation run lengths.

Standard orientations. Reference monitored points. As discussed above, for every type of molecule present in the simulated system, a standard orientation has to be defined first. Then, for every type of molecule, a family of points, related by symmetry operations of the molecule, has to be identified. For a molecule in the standard orientation, one of these points has to be defined as the reference monitored point. Let us recall the example of a crystal of benzene molecules: the standard orientation is shown on the left in Fig. 3, the family of symmetry-related points consists of the six C atoms, and the C atom with coordinates $(x = 0, y > 0, z = 0)$ is the reference monitored point.

Rotation matrices. Sequential runs. It is convenient to put every molecule in its standard orientation at startup, and to describe the orientational state of molecule i by a rotation matrix R_i, so that at any time during the simulation, the current position $\vec{r}'$ of an atom (or any point rotating along) of the molecule is obtained as $\vec{r}' = R_i \vec{r}$, where $\vec{r}$ is the atom's position when the molecule is in the standard orientation. This does not prevent to initially put the molecules in random orientations, which is in fact recommended: instead of the identity matrix I every molecule then has an initial rotation matrix of the type $R_{\vec{s}}(\alpha)$ [Eq. (16)] associated with it. During the simulation, if a rotational MC move with rotation matrix $R_{\vec{s}}(\alpha)$ is accepted, the matrix R_i has to be updated to $R_s(\alpha)R_i$. The matrix R_i is an array variable, and at the end of a program run of, say, Q steps, it is stored. When restarting the program, the matrices R_i are reloaded to regenerate the actual molecular orientations. We stress that it is not necessary to store the matrix R_i after every MC step, only at the end of a program run, to allow for a restart. This keeps data storage limited. We recommend to produce a long run of P MC steps by repeatedly running the MC program for Q MC steps. Here, Q is a divisor of P so that $P = LQ$, with P, Q and L integers. The main advantages of restarting, valid in general when performing (MC) simulations, is that one can quickly study preliminary results, and that one can always resort to a previous, backed-up, simulation state in case of a machine crash. An additional advantage is that one can add features to the program without losing the simulation history. Finally, the memory required for storage can be easily reduced by reducing Q.

Dynamic monitored points. When equilibrium has set in, the sampling of OMSDs (and other quantities) can be started with. First, as explained above, the monitored points have to be reset. This is best done in a separate routine `reset`. For every molecule, the point closest to the reference monitored point has to be identified, and marked as the dynamic monitored point $\vec{r}_i$. Typically, the result of this marking is an index referring to a specific atom (bond, ...) of molecule i. In Fig. 2, for the benzene example, the dynamic monitored point for molecule i has to be identified with C_6 and for molecule j with C_4. OMSDs are calculated using the dynamic monitored point.

OMSDs. After each MC step p, the distance squared $u_i(p)^2$ [Eq. (1)] is calculated and stored for every molecule i.[1] After the first run (let us call it the $l = 1$ run) of Q steps after resetting the monitored points, the OMSDs are obtained as

$$\langle u_i^2 \rangle^{l=1} = \langle u_i^2 \rangle' = \frac{1}{Q} \sum_{p=1}^{Q} u_i(p)^2. \tag{17}$$

Here, the apostrophe refers to the last set of Q values while the superscript l refers to the total set of $P = lQ$ simulation steps; the two sets obviously coincide for $l = 1$. This calculation is best done in a separate routine `process`. After a second run ($l = 2$) of Q steps (without having reset the monitored points, otherwise it would again be a $l = 1$ run), the OMSDs resulting from the second run only have to be calculated first:

$$\langle u_i^2 \rangle' = \frac{1}{Q} \sum_{p=1}^{Q} u_i(p)^2. \tag{18}$$

The overall OMSDs, combining the $l = 1$ and $l = 2$ runs, are then obtained as

$$\langle u_i^2 \rangle^{l=2} = \frac{1}{2} \langle u_i^2 \rangle' + \frac{1}{2} \langle u_i^2 \rangle^{l=1}. \tag{19}$$

In general, after L runs of Q MC steps each, and without resetting the monitored points between runs, the overall OMSDs, based on $P = LQ$ MC simulation steps, read

$$\langle u_i^2 \rangle^{l=L} = \frac{1}{L} \langle u_i^2 \rangle' + \frac{L-1}{L} \langle u_i^2 \rangle^{l=L-1}, \tag{20}$$

where $\langle u_i^2 \rangle'$ is the OMSD based on the last (L-th) run of Q steps only. In Fig. 4, the whole procedure is illustrated schematically. In this way, not the whole series of $u_i(p)^2$ values has to be stored, but only the last sequence. Simulation runs of Q MC steps can be added infinitely, while the required amount for storage memory remains constant. The `reset` routine should

---

[1] In principle, a MC simulation can be performed without storing any sampled quantities. In the case of squared distances, for example, it suffices to add all values of $u_i(p)^2$ during the simulation and to divide the resulting sum by the number of samples afterwards. When one does store sampled values like $u_i(p)^2$, one has the choice to store them in an array variable, or to write them to disk. Storing (the last set of Q) samples has the advantage of having a "history" one can examine for debugging or physical understanding purposes. Particularly important is the evolution of the energy, which should not decrease when equilibrium has set in. Which programming style to use should depend on which optimization level one wants to achieve, which further depends on machine parameters (e.g. RAM and disk memory, I/O management, ...), and on personal taste. We leave it up to the reader to decide which style to use. To illustrate the concept of OMSDs in a clear way, we have opted for a description where sampled quantities are stored.

reset the counter l to 1. The `process` routine calculates $\langle u_i^2 \rangle'$ and $\langle u_i^2 \rangle^l$ and increments l to $l+1$. Note that this way of updating average values based on the previous average value and on the last set of additionally calculated values can be applied to any sampled quantity (e.g. total energy, molecular translational mean-squared displacements, ...).
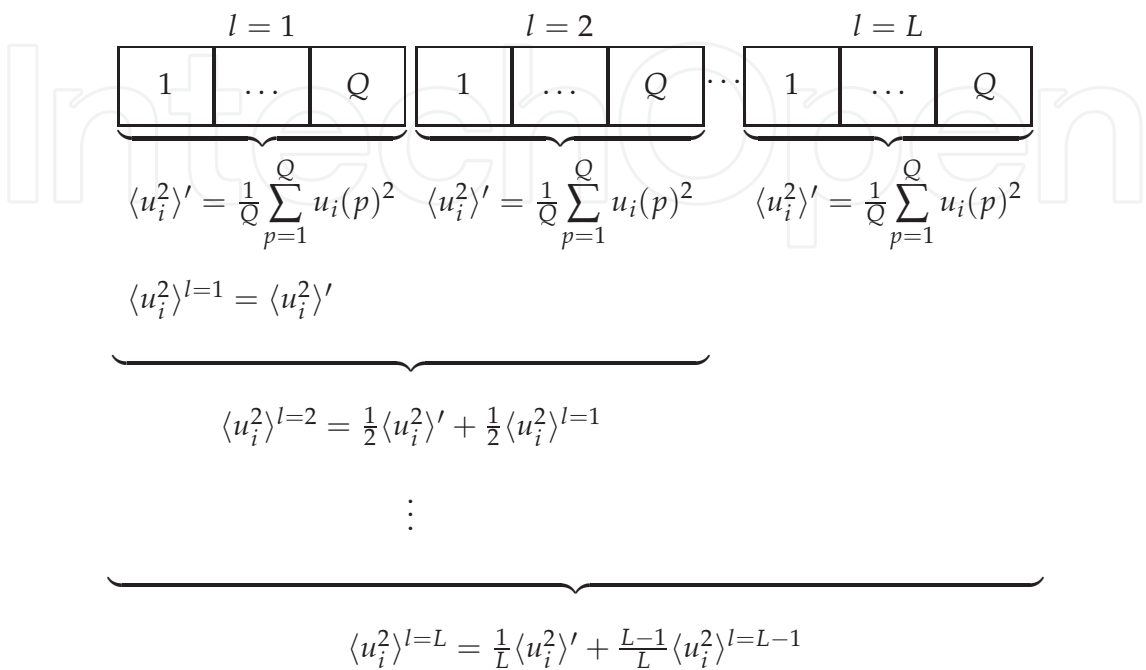

Fig. 4. Scheme for calculating OMSDs based on $P = LQ$ MC simulation steps arising from repeated runs of Q simulation steps.

4. Case studies

After having introduced OMSDs and their practical implementation, we illustrate the usefulness of the concept with two examples involving rotating fullerenes: a 3D crystal containing C_{60} molecules, and a chain of one-dimensionally confined C_{70} molecules. Apart from applying the procedures discussed in the preceding sections, we add some extensions to the OMSD method along the way.

4.1 Fullerene-cubane: orientational ordering in a molecular crystal of C_{60} molecules

Fullerene-cubane, consisting of C_{60} and C_8H_8 molecules, is a unique example of a molecular crystal combining highly symmetrical — icosahedral and cubic — molecules with stoechiometry 1:1 [Pekker et al. (2005)]. At room temperature the crystal lattice is face-centered cubic with the fullerene molecules rotating freely, while below $T \approx 140$ K they adopt fixed orientations within an orthorhombic lattice. The cubane molecules do not rotate in both the high- and the low-T phase, their faces are aligned with the crystal planes. Note that by "fixed orientations" the absence of molecular reorientations is understood; thermal librations are of course present (and are actually reproduced in MC simulations as will be seen from the OMSD values shown below).

In Verberck et al. (2009), an isothermal-isobaric (NpT-ensemble) MC simulation with simple Lennard-Jones pair interactions is reported, and the concept of OMSDs as outlined in the preceding sections is used to study the rotational behavior of the C_{60} (and C_8H_8) molecules upon cooling from $T = 300$ K to 50 K. Here we give an outline of how the OMSD treatment for the C_{60} molecules in fullerene-cubane is set up, and briefly discuss the results. For full details and an interpretation of the results in its physical context we refer to Verberck et al. (2009). The standard orientation is shown in Fig. 5(a): three two-fold symmetry axes of the icosahedral C_{60} molecule coincide with the coordinate axes. The set of equivalent monitored points is chosen to be the set of the 30 double bonds (fusing hexagons of the soccer-ball shaped molecule). The double bond with coordinates $(0, 0, z_d = 3.48$ Å$)$ — for a molecule in the standard orientation, as the definition requires — serves as the reference monitored point [Fig. 5(b)]. Finally, the fixed point $\vec{r}_0$ is chosen to coincide with the reference monitored point. We stress that the fixed and reference monitored points do not necessarily have to be the same.
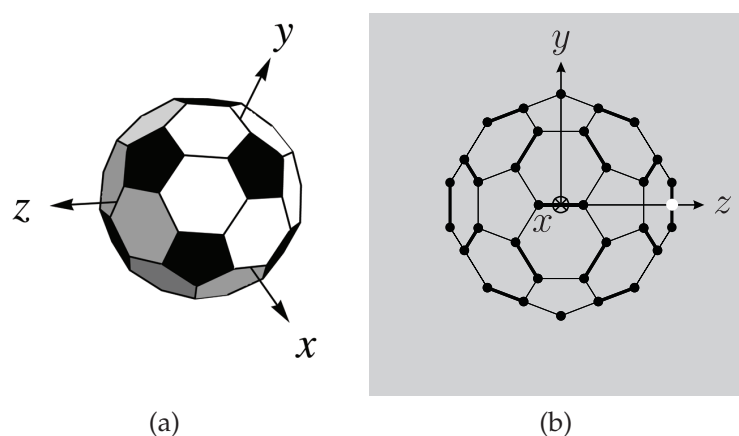

(a)   (b)

Fig. 5. (a) A C_{60} molecule, represented as a soccer ball with 12 pentagons (black) and 20 hexagons (white and shaded), in the standard orientation. (b) Projection onto the (y, z)-plane of a C_{60} molecule in the standard orientation. Double carbon-carbon bonds are shown thicker than single bonds. The double bond with coordinates $(0, 0, z_d = 3.48$ Å$)$ is marked by a white dot.

As stressed above, a reset to determine the dynamic monitored point $\vec{r}_i$ is required before starting the sampling sequence of P MC steps. In the present example, the dynamic monitored point $\vec{r}_i$ for molecule i is its double bond closest to the reference monitored point $(0, 0, z_d = 3.48$ Å$)$.

Since the fixed point has vanishing x- and y-components, the analytical OMSDs for free 3D rotation and no rotation are $r_i^2 + z_d^2$ and $r_i^2 - 2r_i z_d \cos \theta_i + z_d^2$, respectively (see Table 1), which reduce to

$$\langle u_i^2 \rangle_a = 2z_d^2 = 24.22 \text{ Å} \qquad\qquad \text{(free 3D rotation)} \qquad\qquad (21a)$$

and

$$\langle u_i^2 \rangle_a = 2z_d^2 (1 - \cos \theta_i), \qquad\qquad \text{(fixed orientation)} \qquad\qquad (21b)$$

respectively, since $r_i = |\vec{r}_i| = z_d$. We recall that $|\vec{r}_i|$ is indeed independent of the molecular index i, since the standard orientation and the reference monitored point are the same for every molecule.

As remarked already, working with only one fixed point $\vec{r}_0$ is not enough to uniquely characterize the orientational regime. Here, for example, a fixed orientation with $\theta_i = \pi/2$

results in the same OMSD value as for free 3D orientation. Note, however, that in this specific case, a fixed orientation with $\theta_i = \pi/2$ is impossible since then another double bond would be closer to the reference monitored point, which would then instead have had to be set as the dynamic monitored point at reset. In fact, due to the high symmetry of the C_{60} molecule, implying high numbers of equivalent points (e.g. the 30 double bonds), the dynamic monitored point — in the case of no rotation or small librations — will always be close to the reference dynamic monitored point. Consequently, there is an upper limit for the highest value of θ_i. Taking the atomic coordinates of the C_{60} molecule into account, the maximal value for θ_i is about $36°$. (For the benzene example of the previous section, which is easier to visualize, the maximal angle θ_i is $360°/6 = 60°$ — see Fig. 3.)

In Verberck et al. (2009) the average of the dynamic monitored point was used as an alternative fixed point $\vec{r}_0$. We will label the OMSD values resulting from such a type of "dynamic fixed point" as type II OMSDs, and call the OMSDs based on "static fixed points", as in the original definition of Sect. 2, type I OMSDs, and use superscripts ^{I} and ^{II} for labeling the associated OMSD values. For type II OMSDs, the distances to be sampled are of the type

$$u_i(p)^2 = |\vec{r}_i(p) - \langle\vec{r}_i\rangle|^2 = [x_i(p) - \langle x_i\rangle]^2 + [y_i(p) - \langle y_i\rangle]^2 + [z_i(p) - \langle z_i\rangle]^2, \quad (22)$$

with

$$\langle\vec{r}_i\rangle = (\langle x_i\rangle, \langle y_i\rangle, \langle z_i\rangle) = \frac{1}{P}\sum_{p=1}^{P}\vec{r}_i(p). \quad (23)$$

At first sight, this requires to store all $\vec{r}_i(p) = (x_i(p), y_i(p), z_i(p))$ values until the very end of the whole series of $L = P/Q$ simulation runs of Q MC steps each, and that only then $\langle\vec{r}_i\rangle$ and $\langle u_i^2\rangle = \frac{1}{P}\sum_{p=1}^{P}u_i(p)^2$ can be calculated. However, applying the usual "trick" for the evaluation of standard deviations in statistics,

$$\begin{aligned}
\langle u_i^2\rangle^{II} &= \frac{1}{P}\sum_{p=1}^{P}u_i(p)^2 \\
&= \frac{1}{P}\sum_{p=1}^{P}\left([x_i(p) - \langle x_i\rangle]^2 + [y_i(p) - \langle y_i\rangle]^2 + [z_i(p) - \langle z_i\rangle]^2\right) \\
&= \frac{1}{P}\sum_{p=1}^{P}(x_i(p)^2 - 2x_i(p)\langle x_i\rangle + \langle x_i\rangle^2 + y_i(p)^2 - 2y_i(p)\langle y_i\rangle + \langle y_i\rangle^2 \\
&\qquad + z_i(p)^2 - 2z_i(p)\langle z_i\rangle + \langle z_i\rangle^2) \\
&= \langle x_i^2\rangle - \langle x_i\rangle^2 + \langle y_i^2\rangle - \langle y_i\rangle^2 + \langle z_i^2\rangle - \langle z_i\rangle^2 \\
&= \langle r_i^2\rangle - \langle x_i\rangle^2 - \langle y_i\rangle^2 - \langle z_i\rangle^2 \\
&= z_d^2 - \langle x_i\rangle^2 - \langle y_i\rangle^2 - \langle z_i\rangle^2, \quad (24)
\end{aligned}$$

shows that storing the coordinates $x_i(p)$, $y_i(p)$ and $z_i(p)$ during a simulation sequence of Q steps suffices. Indeed, the squares of the averages $\langle x_i\rangle$, $\langle y_i\rangle$ and $\langle z_i\rangle$ are used to calculate the OMSD value $\langle u_i^2\rangle^{l=1} = \langle u_i^2\rangle' = \sum_{p=1}^{Q}u_i(p)^2$ based on the first simulation run of Q MC steps, which is then updated each time a sequence of Q MC steps is added according to the scheme

shown in Fig. 4. Again, the required computer memory remains constant (and can be reduced by reducing Q), while segments of Q MC steps can be added ad libitum. Note that when using a static fixed point, i.e. a point $\vec{r}_0 = (x_0, y_0, z_0)$ that does not "dynamically" depend on the simulation itself, the same approach involving the storing of the coordinates of $\vec{r}_i$ can be used. Rather than calculating and storing the distance squared $u_i(p)^2$ [Eq. (1)] after each MC step and averaging at the end, one can calculate the averages $\langle x_i \rangle$, $\langle y_i \rangle$ and $\langle z_i \rangle$ and use the formula

$$\langle u_i^2 \rangle^{\mathrm{I}} = z_{\mathrm{d}}^2 - 2\langle x_i \rangle x_0 - 2\langle y_i \rangle y_0 - 2\langle z_i \rangle z_0 + r_0^2. \tag{25}$$

This approach can be considered when combining the two types of fixed points (static or dynamic) since for type II OMSDs $\langle x_i \rangle$, $\langle y_i \rangle$ and $\langle z_i \rangle$ have to be calculated anyway. An important property of type II OMSDs is that they vanish in the case of fixed orientations, which follows trivially from $\vec{r}_i(p) = \langle \vec{r}_i \rangle_{\mathrm{a}}$:

$$\langle u_i^2 \rangle_{\mathrm{a}}^{\mathrm{II}} = 0 \qquad \text{(fixed orientation)}. \tag{26}$$

Note that this property complements the orientation-dependent outcome of $\langle u_i^2 \rangle_{\mathrm{a}}^{\mathrm{I}}$ [Eq. (21b)]. For free rotation, $\langle \vec{r}_i \rangle_{\mathrm{a}} = \vec{0}$, so that

$$\langle u_i^2 \rangle_{\mathrm{a}}^{\mathrm{II}} = \langle |\vec{r}_i|^2 \rangle_{\mathrm{a}} = z_{\mathrm{d}}^2 = 12.11 \text{ Å}^2 \qquad \text{(free 3D orientation)}. \tag{27}$$
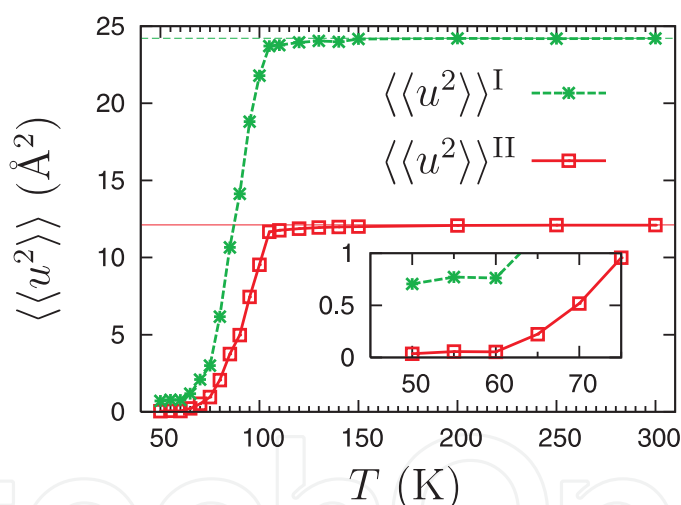

Fig. 6. Averaged type I and type II OMSD values $\langle\langle u^2 \rangle\rangle^{\mathrm{I}}$ and $\langle\langle u^2 \rangle\rangle^{\mathrm{II}}$ for C_{60} molecules in fullerene-cubane as a function of temperature T. The 300 K values correspond to the free rotation values of $2z_{\mathrm{d}}^2 = 24.22$ Å^2 and $z_{\mathrm{d}}^2 = 12.11$ Å^2, respectively (shown by horizontal lines).

The type I and type II OMSD values resulting from the simulation, averaged over all molecules, written as $\langle\langle u^2 \rangle\rangle^{\mathrm{I}}$ and $\langle\langle u^2 \rangle\rangle^{\mathrm{II}}$ [see Eq. (3)], respectively, are shown in Fig. 6 as a function of temperature T. They nicely show a transition from freely rotating to orientationally frozen molecules. Indeed, the 300 K values match the exact analytical values of z_{d}^2 and $2z_{\mathrm{d}}^2$, while at 50 K, $\langle\langle u^2 \rangle\rangle^{\mathrm{II}} \approx 0$, implying fixed molecular orientations. The small deviations of $\langle\langle u^2 \rangle\rangle^{\mathrm{II}}$ from zero (see Inset of Fig. 6) are a consequence of thermally induced librations. The transition covers the temperature range $65 \text{ K} \lesssim T \lesssim 110 \text{ K}$, which can be interpretated as a
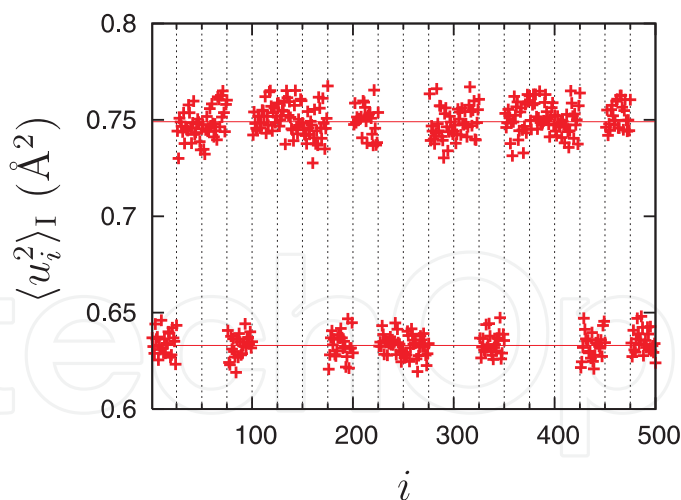
Fig. 7. Molecular $\langle u_i^2 \rangle^{\mathrm{I}}$ OMSD values of the 500 C_{60} molecules in the simulation box, at $T = 50$ K. Two groups of molecules, with values around 0.633 Å^2 and 0.749 Å^2 (shown by horizontal lines), are clearly distinguishable.

slow freezing of the rotational motion, and could be observed experimentally as a continuous diminishing of diffuse x-ray scattering.

The finite low-T values of $\langle \langle u^2 \rangle \rangle^{\mathrm{I}}$ correspond to specific fixed molecular orientations. It is, however, wrong to a priori assume that all molecules adopt the same orientation. The individual molecular $\langle u_i^2 \rangle^{\mathrm{I}}$ values have to be examined to conclude upon the precise molecular orientations. In Fig. 7, the $T = 50$ K $\langle u_i^2 \rangle^{\mathrm{I}}$ values for the 500 C_{60} molecules in the simulation box are shown. Interestingly, the values can be divided into two groups, with average values $\langle u_i^2 \rangle^{\mathrm{I}} \approx 0.633$ Å^2 and $\langle u_i^2 \rangle^{\mathrm{I}} \approx 0.749$ Å^2, corresponding to two classes of molecular orientations. The details of the determination of the molecular orientations resulting in Fig. 7 fall beyond the scope of the present Chapter; for a complete analysis we refer to Verberck et al. (2009). We do point out, however, that it turns out useful to keep track of the averages $\langle x_i \rangle$, $\langle y_i \rangle$ and $\langle z_i \rangle$ since they help to deduce the molecules' orientations. Indeed, knowledge of $\langle \vec{r}_i \rangle$ already fixes the i-th molecule's average orientation up to a rotation about the vector $\langle \vec{r}_i \rangle$. Note that this requires almost no extra programming and memory since averages of the dynamic monitored points' coordinates have already been included in the implementation of type II OMSDs [cfr. Eq. (24)].

4.2 Nanopeapods: orientational behaviour in one-dimensional chains of C_{70} molecules

Our second example illustrating the concept of OMSDs is a chain of C_{70} molecules encapsulated in a CNT. Such a system falls into the category of so-called nanopeapods, nanotubes filled with atom or molecules. Historically, the insertion of C_{60} molecules was reported first [Smith et al. (1998)], but many other peapod systems have been synthesized and investigated by now. For a review, we refer to Monthioux (2002).

One of the interesting properties of C_{70}@CNT systems is the dependence of the molecule's orientation on the tube radius R: for a small radius, the molecules adopt lying orientations [Fig. 8(a)] while for larger R, molecules adopt standing orientations [Fig. 8(b)]. Obviously, this a consequence of the molecule's geometry and its van der Waals interaction with the surrounding nanotube. Recently, a canonical-ensemble (NVT) MC simulation of C_{70} peapods in a CNT modelled as a homogeneous carbonic cylinder was carried out in order to study the temperature and the and radius dependence of the molecular motion of the one-dimensionally

confined fullerene molecules [Verberck et al. (2011)]. In particular, OMSDs were used to characterize the molecules' rotational behavior. Here, as in the previous subsection, we discuss how the OMSD analysis is set up, and point to possible additions.
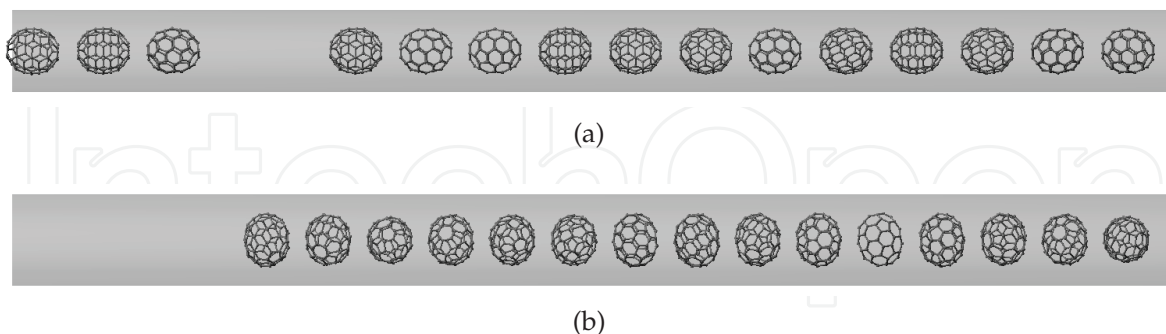

(a)

(b)

Fig. 8. Carbon nanotubes filled with C_{70} molecules. (a) For a tube radius of 6.5 Å, the molecules adopt lying orientations (the molecule's long axis parallel to molecule's long axis). (b) For a radius of 7.3 Å, the molecules adopt standing orientations (at sufficiently low temperatures).

As a first step, a standard orientation for the investigated molecules has to be defined. The C_{70} standard orientation is shown in Fig. 9; it is a lying orientation. Next, a set of equivalent monitored points has to be identified. A convenient choice is the pair of top and bottom pentagons' centers $(0, 0, \pm z_p)$, with $z_p = 3.99$ Å. The point with the positive z-coordinate is chosen as the reference monitored point (Fig. 9).
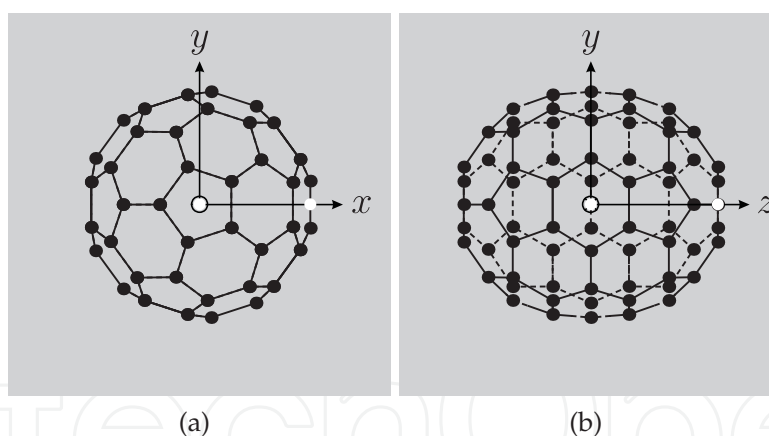

(a)   (b)

Fig. 9. Projections of a C_{70} molecule in the standard orientation on the (a) (x, y)- and the (b) (y, z)-plane. The two reference monitored points $(0, 0, z_t = 3.99$ Å$)$ and $(x_b = 3.49$ Å$, 0, 0)$ are marked by white dots.

Rather than working with type I and type II OMSDs for one fixed point, as in the example of the previous subsection, only type II OMSDs were used in Verberck et al. (2011), but for two monitored points. We therefore introduce superscripts ^{II,1} and ^{II,2}. The second set of monitored points is the ring of five bonds in the equatorial plane ($z = 0$) of the C_{70} molecule in the standard orientation; the point $(x_b, 0, 0)$ with $x_b = 3.49$ Å is set as the second reference monitored point (Fig. 9). For free 3D rotations, we have — see the previous subsection —

$\langle u_i^2 \rangle_a^{\text{II}} = \langle |\vec{r}_i|^2 \rangle_a$ so that the type II OMSDs read

$$\langle u_i^2 \rangle_a^{\text{II},1} = z_t^2 = 15.90 \text{ Å}^2 \qquad \text{(free 3D orientation)}, \qquad (28a)$$

$$\langle u_i^2 \rangle_a^{\text{II},2} = x_b^2 = 12.15 \text{ Å}^2 \qquad \text{(free 3D orientation)}. \qquad (28b)$$

For fixed orientations, the OMSDs vanish:

$$\langle u_i^2 \rangle_a^{\text{II},1} = 0 \qquad \text{(no rotation)}, \qquad (29a)$$

$$\langle u_i^2 \rangle_a^{\text{II},2} = 0 \qquad \text{(no rotation)}. \qquad (29b)$$

Another case of interest is free molecular rotation about the z-axis (cfr. Sect. 2). Using the appropriate average for this case, Eq. (8), one easily obtains

$$\langle \vec{r}_i \rangle_a = \left\langle (r_i \sin\theta_i \cos\phi_i, r \sin\theta_i \sin\phi_i, r \cos\theta_i) \right\rangle_a = (0, 0, r_i \cos\theta_i), \qquad (30)$$

so that, using Eq. (24),

$$\langle u_i^2 \rangle_a^{\text{II}} = r_i^2 (1 - \cos^2\theta_i), \qquad (31)$$

resulting in

$$\langle u_i^2 \rangle_a^{\text{II},1} = z_t^2 (1 - \cos^2\theta_i) \qquad \text{(free z-orientation)}, \qquad (32a)$$

$$\langle u_i^2 \rangle_a^{\text{II},2} = x_b^2 (1 - \cos^2\theta_i) \qquad \text{(free z-orientation)}. \qquad (32b)$$

The polar angle of the first dynamic monitored point equals 0 for lying and $\pi/2$ for standing molecules, respectively, so that

$$\langle u_i^2 \rangle_a^{\text{II},1} = 0 \qquad \text{(lying, free z-orientation)}, \qquad (33a)$$

$$\langle u_i^2 \rangle_a^{\text{II},1} = z_t^2 \qquad \text{(standing, free z-orientation)}. \qquad (33b)$$

For the second dynamic monitored point $\theta_i = \pi/2$ for any lying orientation. For standing orientations, the value of θ_i can adopt any value between 0 and π, depending on the molecule's orientation with respect to its own long axis. Hence

$$\langle u_i^2 \rangle_a^{\text{II},2} = x_b^2 \qquad \text{(lying, free z-orientation)}, \qquad (34a)$$

$$\langle u_i^2 \rangle_a^{\text{II},2} = x_b^2 (1 - \cos^2\theta_i) \qquad \text{(standing, free z-orientation)}. \qquad (34b)$$

It can be shown that in the case of a standing molecule, rotating freely about the z-axis and freely about its long axis (i.e. spinning freely), $\langle \cos^2\theta_i \rangle = 0$ for the second dynamic monitored point, so that

$$\langle u_i^2 \rangle_a^{\text{II},2} = x_b^2 \qquad \text{(standing, free z-orientation, free spinning)}. \qquad (35)$$

The various cases are summarized in Table 2.

It follows that only lying molecules rotating freely about the z-axis and absence of molecular rotation can be unambiguously inferred from the pair $(\langle u_i^2 \rangle_a^{\text{II},1}, \langle u_i^2 \rangle_a^{\text{II},2})$. Free 3D rotations and free rotations about the z-axis in combination with free spinning of the molecule about its long axis result in the same OMSDs. The case of free z-rotation of a standing molecule, not spinning about its long axis, and with a fixed polar angular value of $\theta_i = \pi/2$ for the second

			$\langle u_i^2 \rangle_a^{\text{II},1}$	$\langle u_i^2 \rangle_a^{\text{II},2}$
free 3D rotation			$z_t^2 = 15.90$ Å^2	$x_b^2 = 12.15$ Å^2
free z-rotation	lying		0	x_b^2
	standing	free spinning	z_t^2	x_b^2
		no spinning	z_t^2	$x_b^2(1 - \cos^2\theta_i)$
no rotation			0	0

Table 2. Analytical OMSD values $\langle u_i^2 \rangle_a^{\text{II},1}$ and $\langle u_i^2 \rangle_a^{\text{II},2}$ for reference monitored points $(0, 0, z_t)$ and $(x_b, 0, 0)$, respectively, for several cases of interest.

dynamic monitored point, also results in the same pair of OMSDs. This accidental coincidence can be easily resolved, though, by considering a third monitored point (e.g. any other bond in the equatorial belt of the C_{70} molecule, see Fig. 9). On the other hand, the coincidence for free 3D rotation and free z-rotation plus free spinning is hard to lift using OMSDs only. A simpler solution, described in Verberck et al. (2011) is to monitor the z-coordinate of the first dynamic monitored point. Indeed, for free 3D rotation, its value should be uniformly distributed in the interval $[-z_t, z_t]$, while for a permanently standing molecule (regardless of whether it rotates about the z-axis and/or spins about its long axis) its value should be 0. To extract the distribution of z-coordinate values in a MC simulation, it is necessary to make a histogram. This can be either done on-the-fly, by incrementing the bin count of the bin corresponding to the current z-coordinate, or in the `process` routine if the z_i values of the dynamic monitored point are stored during the simulation.
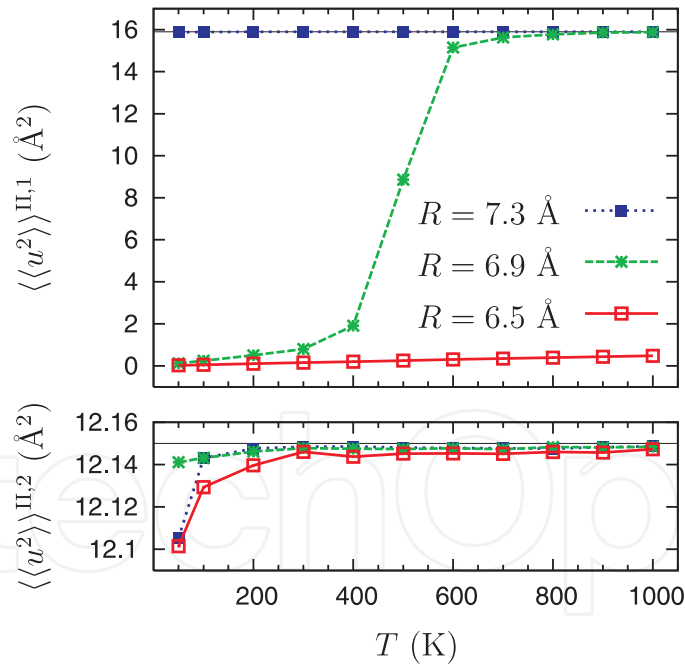

Fig. 10. Averaged type II OMSD values $\langle\langle u^2 \rangle\rangle^{\text{II},1}$ and $\langle\langle u^2 \rangle\rangle^{\text{II},2}$ for C_{70} nanopeapods with three different radii R, as a function of temperature T. The free rotation values of $z_t^2 = 15.90$ Å^2 and $x_b^2 = 12.15$ Å^2 are shown by horizontal lines.

In Fig. 10, the OMSDs $\langle u_i^2 \rangle_a^{\text{II},1}$ and $\langle u_i^2 \rangle_a^{\text{II},2}$, averaged over all (15) molecules, resulting from the MC simulation are shown for three different radii, as a function of temperature. The smallest tube radius, $R = 6.5$ Å, features lying molecules, freely rotating about the long axis of the

tube (z-axis). At low temperatures, judging from the values of $\langle u_i^2 \rangle_a^{II,2}$ being slighly smaller than x_b^2, the free character of the rotations is only almost reached, which can be attributed to intermolecular interactions favoring specific mutual orientations. At high temperatures, truly free rotation has been achieved, but now the small deviation of $\langle u_i^2 \rangle_a^{II,1}$ from zero suggests thermal fluctuations — very small tilts away from the ideal lying orientation.

For the highest radius, $R = 7.3$ Å, the OMSD values imply that molecules rotate freely, either three-dimensionally or around the z-axis (with spinning). The procedure involving histograms of the z-coordinates of the first dynamic monitored point mentioned above reveals a transition from standing molecules at low temperatures to complex 3D rotations at higher temperatures. For details, we refer to Verberck et al. (2011).

The intermediate radius $R = 6.9$ Å shows a transition from quasi-freely (cfr. $R = 6.5$ Å) z-rotating lying molecules to — as follows from the z-coordinate histogram analysis — a complex pattern of 3D molecular rotations.

5. Summary

In the present Chapter, we have introduced a method to quantify molecular rotational motion in molecular crystals, and have shown how to embed it in a typical MC simulation. The key concept is that of OMSDs, a rotational analogue of translational mean-squared displacements. By carefully choosing a point that rotates along with a molecule, following it during the simulation, and calculate its distance squared to a fixed point, a measure for the "degree of rotation" of the molecule is obtained. We have shown how to properly set up this procedure to avoid biassed results due to the initial equilibrating phase and due to molecular symmetry. Also, we discussed practical issues required for the efficient implementation of the OMSD technique.

Two examples of MC simulations where OMSDs were used — a 3D molecular crystal consisting of C_{60} molecules and a 1D arrangement of C_{70} molecules in a nanotube — were covered. The examples show the power of the OMSD method. By combining two types of OMSDs and using more than one monitored point, it is possible to deduce the rotational regimes of the molecules in a simulation box. Typical regimes are free 3D rotations, free rotations about an axis, or no rotations. In the latter case, the examination of OMSD values helps to determine the actual molecular orientations. The examples also provide hints to resolve occasional ambiguities. Indeed, some types of rotational motion can be indistinguishable within a certain set of OMSDs. In these cases, looking at average values or histograms of coordinates of the monitored point(s) — which requires minimal additional programming since these are parameters already required for the calculation of OMSDs — or extending the set of OMSDs can resolve the problem.

For completeness, we point out that the procedures described in the preceding sections can be easily extended to the case of a crystal of several types of molecules. It simply suffices to define a standard orientation, monitored points (reference and dynamic) and fixed points for each type of molecule, and to process the several molecular sublattices separately.

In summary, the OMSD method provides a way to map the huge number of variables (atomic coordinates) in a MC simulation of a molecular crystal onto a very small set of quantities completely describing the molecule's rotational motion.

Acknowledgements

6. References

Allen, M.P. & Tildesley, D.J. (1987). *Computer Simulation of Liquids*, Oxford University Press, ISBN 0-19-855645-4, Oxford

Frenkel, D. & Smit, B. (2002). *Understanding Molecular Simulation: From Algorithms to Applications*, 2nd Ed., Academic Press, ISBN 0-12-267351-4, San Diego

Lynden-Bell, R.M. & Michel, K.H. (1994). Translation–rotation coupling, phase transitions, and elastic phenomena in orientationally disordered crystals. *Reviews of Modern Physics*, 66, 3 (July 1994) (721-762), ISSN 0034-6861

Miles, R.E. (1965). On random rotations in $\mathbb{R}^3$. *Biometrika*, 52, 3/4 (December 1965) (636-639), ISSN 0006-3444

Monthioux, M. (2002). Filling single-wall carbon nanotubes. *Carbon*, 40, 10 (August 2002) (1809-1823), ISSN 0008-6223

Pekker, S.; Kováts, É.; Oszlányi, G.; Bényei, G.; Klupp, G.; Bortel, G.; Jalsovszky, I.; Jakab, E.; Borondics, F.; Kamarás, K.; Bokor, M.; Kriza, G.; Tompa, K. & Faigel, G. (2005). Rotor–stator molecular crystals of fullerenes with cubane. *Nature Materials*, 4, 10 (September 2005) (764-767), ISSN 1476-1122

Smith, B.W.; Monthioux, M. & Luzzi, D.E. (1998). Encapsulated C_{60} in carbon nanotubes. *Nature*, 396, 6709, (26 November 1998) (323-324), ISSN 0028-0836

Verberck, B.; Vliegenthart, G.A. & Gompper, G. (2009). Orientational ordering in solid C_{60} fullerene-cubane. *The Journal of Chemical Physics*, 130, 15 (21 April 2009) (154510.1-14), ISSN 0021-9606

Verberck, B.; Cambedouzou, J.; Vliegenthart, G.A.; Gompper, G. & Launois, P. (2011). Molecular motion in C_{70}@SWCNT nanopeapods: a Monte Carlo study. Accepted for publication in *Carbon*, ISSN 0008-6223

Vesely, F.Z. (1982). Angular Monte Carlo Integration Using Quaternion Parameters: A Spherical Reference Potential for CCl_4. *Journal of Computational Physics*, 47, 2 (August 1982) (291-296), ISSN 0021-9991

Applications of Monte Carlo Method in Science and Engineering
Edited by Prof. Shaul Mordechai

ISBN 978-953-307-691-1
Hard cover, 950 pages
Publisher InTech
Published online 28, February, 2011
Published in print edition February, 2011

In this book, Applications of Monte Carlo Method in Science and Engineering, we further expose the broad range of applications of Monte Carlo simulation in the fields of Quantum Physics, Statistical Physics, Reliability, Medical Physics, Polycrystalline Materials, Ising Model, Chemistry, Agriculture, Food Processing, X-ray Imaging, Electron Dynamics in Doped Semiconductors, Metallurgy, Remote Sensing and much more diverse topics. The book chapters included in this volume clearly reflect the current scientific importance of Monte Carlo techniques in various fields of research.

INTECH
open science | open minds